CRITICAL EXAMINATIONS OF QSO REDSHIFT PERIODICITIES AND ASSOCIATIONS WITH GALAXIES IN SLOAN DIGITAL SKY SURVEY DATA

SU MIN TANG[1] AND SHUANG NAN ZHANG[1,2,3,4]

ABSTRACT

We have used the publicly available data from the Sloan Digital Sky Survey and 2dF QSO redshift survey to test the hypothesis that QSOs are ejected from active galaxies with periodic noncosmological redshifts. For two different intrinsic redshift models, namely the Karlsson $\log(1 + z)$ model and Bell's decreasing intrinsic redshift (DIR) model, we do two tests. First, using different criteria, we generate four sets of QSO-galaxy pairs and find there is no evidence for a periodicity at the predicted frequency in $\log(1 + z)$, or at any other frequency. We then check the relationship between high-redshift QSOs and nearby active galaxies, and we find that the distribution of projected distance between high-redshift QSOs and nearby active galaxies and the distribution of redshifts of those active galaxies are consistent with a distribution of simulated random pairs, completely different from Bell's previous conclusion. We also analyze the periodicity in redshifts of QSOs, and no periodicity is found in high-completeness samples, contrary to the DIR model. These results support the hypothesis that QSOs are not ejected from active galaxies.

Subject headings: galaxies: active — large-scale structure of universe — quasars: general

1. INTRODUCTION

The debate on whether quasi-stellar objects (QSOs) are ejected from the nuclei of low-redshift galaxies with a periodic noncosmological "intrinsic" redshift has been going on for many years. Some evidence has been claimed to suggest such an intrinsic redshift hypothesis, in which QSOs have redshifts that are much larger than their parent galaxies and the excess of redshift is assumed to represent an always redshifted intrinsic component (Burbidge & Burbidge 1967; Arp et al. 1990, 2005; Karlsson 1990; Chu et al. 1998; Burbidge & Napier 2001; Bell 2004).

Two models have been discussed in the literature that predict exact values for the preferred redshifts. One of these is the Karlsson formula, which suggests a periodicity of $\Delta \log(1 + z_{\rm eff}) = 0.089$ with peaks lying at 0.061, 0.30, 0.60, 0.96, 1.14, 1.96, and so on (Karlsson 1977, 1990; Arp et al. 1990, 2005; Burbidge & Napier 2001; Napier & Burbidge 2003), where $z_{\rm eff}$ is the redshift of the QSO measured relative to the nearby galaxy, called effective redshift, which is defined as

$$1 + z_{\rm eff} = (1 + z_Q)/(1 + z_G), \qquad (1)$$

where z_Q is the observed quasar redshift and z_G is the redshift of the associated galaxy that is assumed to be the ejecting galaxy. To explain such a periodicity, they claimed that quasars are ejected by active galaxies and the putative parent galaxies are generally much brighter than their quasar offspring (Arp et al. 2005). As claimed by Burbidge & Napier (2001) and Napier &

Burbidge (2003), the typical projected association separation is about 200 kpc.

Another model, namely the decreasing intrinsic redshift model (DIR model), was proposed by Bell (2004), where the QSO intrinsic redshift equation is given by the relation

$$z_{iQ} = z_f(N - M_N), \qquad (2)$$

where $z_f = 0.62 \pm 0.01$ is the intrinsic redshift constant, N is an integer, and M_N varies with N and is a function of a second quantum number n. In the DIR model, galaxies are produced continuously through the entire age of the universe, and QSOs are assumed to be ejected from the nuclei of active galaxies and represent the first very short lived stage (10^7–10^8 yr) in the evolution of galaxies (Bell 2004).

The above intrinsic redshift hypothesis, if true, will have far-reaching consequences for cosmology and the nature of QSOs. Most of those previous studies on the Karlsson formula used rather small samples (except for Arp et al. 2005) and have suspected that the claimed peaks were due to artifacts associated with selection effects (Basu 2005). To avoid such a heterogeneous selection manner as well as personal prejudice, Hawkins et al. (2002) tested the periodicity in $\log(1 + z_{\rm QSO})$ with Two Degree Field (2dF) redshift survey data with 67,291 nearby galaxies and 10,410 QSOs; it was found that there is no periodicity in $\log(1 + z_{\rm QSO})$. However, Napier & Burbidge (2003) argued that in order to use the 2dF sample to properly test the original hypothesis, it is necessary to establish for each pair that the galaxy is at least a late-type active spiral system. Arp et al. (2005) also reexamined the 2dF sample and claimed that they found that the redshifts of brighter QSOs in the QSO density contours fit very exactly the long-standing Karlsson formula and confirm the existence of preferred values in the distribution of quasar redshifts.

In an attempt to resolve these issues, we turn to the Sloan Digital Sky Survey (SDSS) (and also the 2dF QSO Redshift Survey [2QZ] occasionally) to carry out this study, which has the largest homogeneous sample of data, as well as the spectroscopic

[1] Department of Physics and Center for Astrophysics, Tsinghua University, Beijing 100084, China; tangsm99@mails.tsinghua.edu.cn, zhangsn@tsinghua.edu.cn.
[2] Department of Physics, University of Alabama in Huntsville, Optics Building 201C, Huntsville, AL 35899.
[3] Space Science Laboratory, NASA Marshall Space Flight Center, SD50, Huntsville, AL 35812.
[4] Institute of High Energy Physics, Chinese Academy of Sciences, P.O. Box 918-3, Beijing 100039, China.

subclassification of galaxies. In § 2, to test whether there is a periodicity existing in $\log(1+z)$, we construct four sets of QSO-galaxy pairs with different QSOs and galaxies, with all QSOs projected within 200 kpc from nearby galaxies at these galaxies' distances. QSO density contours are also presented to show that there is no periodicity in SDSS QSOs under such analysis. In § 3, we examine the relationship between high-z QSOs and nearby active galaxies to show that such QSOs are not likely to be ejected by nearby active galaxies. In § 4, we analyze the redshift distribution of QSOs in SDSS Data Release 3 (DR3) and 2QZ to show that there is no evidence for nonartificial periodicity in redshifts of QSOs, contrary to the DIR model. A discussion and conclusions are in § 5.

2. NO PERIODICITY IN $\log(1+z)$

2.1. The SDSS Data and Pair Selection

In this section, we use the SDSS Data Release 1 (DR1; Abazajian et al. 2003) QSO catalog (Schneider et al. 2003) and the New York University Value-Added Galaxy Catalog (NYU-VAGC; Blanton et al. 2005). For reliability in the derived redshifts, we consider only those QSOs in the range of $z > 0.4$ and galaxies in the range of $0.01 < z < 0.2$ with the highest plate quality labeled as "good" and with no redshift warning. This quality control leaves a total of 190,591 galaxies and 15,747 QSOs in the sample.

Three issues need to be carefully addressed when we analyze the relation between foreground galaxies and QSOs, as well as the redshift distribution of QSOs, since due to the survey strategies and the instrumental limitations, the selections of galaxies and QSOs are not entirely independent, and the selection of QSOs in SDSS is also dependent on redshift. First, due to the mechanical constraint in SDSS that spectroscopic fibers must be separated by $55''$ on a given plate (Blanton et al. 2003), some QSO-galaxy pairs would be consequently missing from the spectroscopic sample. However, this issue would have little effect on the results for two reasons: (1) $55''$ corresponds to an angular distance of 40 kpc for a galaxy at $z = 0.04$, which is the typical redshift value in our galaxy sample; only a few pairs (about 5%) would be missing in a given separation of 200 kpc for randomly distributed QSOs and galaxies, which is also shown in Figure 7, where the distribution of data pairs is consistent with randomly distributed pairs. (2) Such a fiber constraint is independent of redshifts of galaxies or QSOs; therefore its redshift distribution will not be biased, although some pairs are missing in the sample. Second, the magnitude limits of the SDSS galaxy and QSO spectroscopic surveys are quite different, i.e., $i < 19.1$ for $z < 3$ QSOs, $i < 20.2$ for $z > 3$ QSOs, $r < 17.77$ for most sampled galaxies, and $r < 19.5$ for luminous red galaxies (Richards et al. 2002; Strauss et al. 2002); hence the magnitudes of QSOs are mostly higher than galaxies. However, since in the ejection hypothesis the parent galaxies are generally much brighter than their QSO offspring (Bell 2005; Arp et al. 2005), the pair-making process is not likely to be affected by the magnitude differences between QSOs and galaxies, which are also shown in Figures 12 and 13. Moreover, the fact that the completeness of the spectroscopic selection varies with redshift (Richards et al. 2002) will consequentially affect the redshift distribution of QSOs and might cause artificial periodicities into data, as is discussed extensively in § 4. However, since low-z ($z < 2.5$) QSOs, for which the completeness is uniform and high (>90%; Richards et al. 2002), occupied a very large fraction of all QSOs (about 90%), such selection dependence in redshift would not smear out intrinsic periodicities in QSO redshift if they do exist.

It has been suggested that quasars with bright apparent magnitude will generally be nearby, that the redshifts of these quasars will require little or no correction for the periodicity effects to be manifested, and that those low-redshift galaxies with which such quasars appear to be preferentially associated tend to be morphologically disturbed active galaxies (Arp et al. 2005). Therefore, to make our results more compelling, we select a subsample of 3724 QSOs, called bright QSOs, which have i-band magnitudes less than 18.5, and a subsample of 77,426 galaxies, called active galaxies, which are labeled as star-forming, starburst, star-forming broad-line, or starburst broad-line galaxies in the spectroscopic subclassification. Then with different combinations we construct four sets of QSO-galaxy samples and get four sets of pairs in which a QSO is projected within 200 kpc from a galaxy: 4572 pairs for QSO-nearby galaxies, 3216 pairs for QSO-active nearby galaxies, 1129 pairs for bright QSO-nearby galaxies, and 791 pairs for bright QSO-active nearby galaxies. When there is more than one galaxy within the 200 kpc projected distance limit of the QSO, we take the closest galaxy in projected distance to make up the pair.

2.2. Analysis and Results

We make a power-spectrum analysis to investigate the periodicity hypothesis of Karlsson (1977). The power I is defined as in Burbidge & Napier (2001):

$$I(\nu) = 2R^2/N, \qquad (3)$$

where

$$R^2 = S^2 + C^2, \qquad (4)$$

with

$$S = \sum_{i=1}^{N} w_i \sin(2\pi x_i/P), \quad C = \sum_{i=1}^{N} w_i \cos(2\pi x_i/P), \qquad (5)$$

where $\nu = 1/P$, and $x_i = \log(1+z_i)$. Here w_i is a weighting function, and $w_i \equiv 1$, except in § 4, as in the analysis of Burbidge & Napier (2001). For randomly and uniformly distributed redshifts, $\bar{I} = 2$.

To test our code developed for this study, we first reanalyze the 290 QSOs in the data sets of Karlsson (1990) and Napier & Burbidge (2003), as shown in Figure 1. Errors on $I(P)$ are given by using the bootstrap methods (Efron 1979) in the following steps: (1) we take the nonzero number in each bin in the upper histogram as the expectation value of a Poisson distribution; and (2) we resample each bin following the Poisson distribution to reproduce 1000 new sets of data, repeat the power spectral analysis on these resamplings, and finally calculate the standard deviations in the derived values of I at different periods P. Clearly the periodicity at around $\Delta \log(1 + z_{\rm eff}) = 0.089$ is highly significant at above the 3.5 σ level.

In Figures 2–5 we show histograms of the effective redshifts of QSOs paired with galaxies and their unwindowed power spectra with standard deviations calculated in the same way as for Figure 1. Pairs in these four figures are for QSO-nearby galaxies, QSO-active nearby galaxies, bright QSO-nearby galaxies, and bright QSO-active nearby galaxies, as described in § 2.1. Our results show that for these significantly larger samples than that in Figure 1, all peaks that appeared in the power spectra are
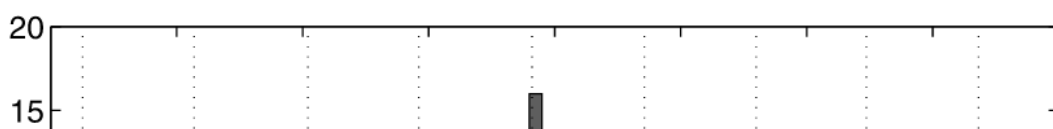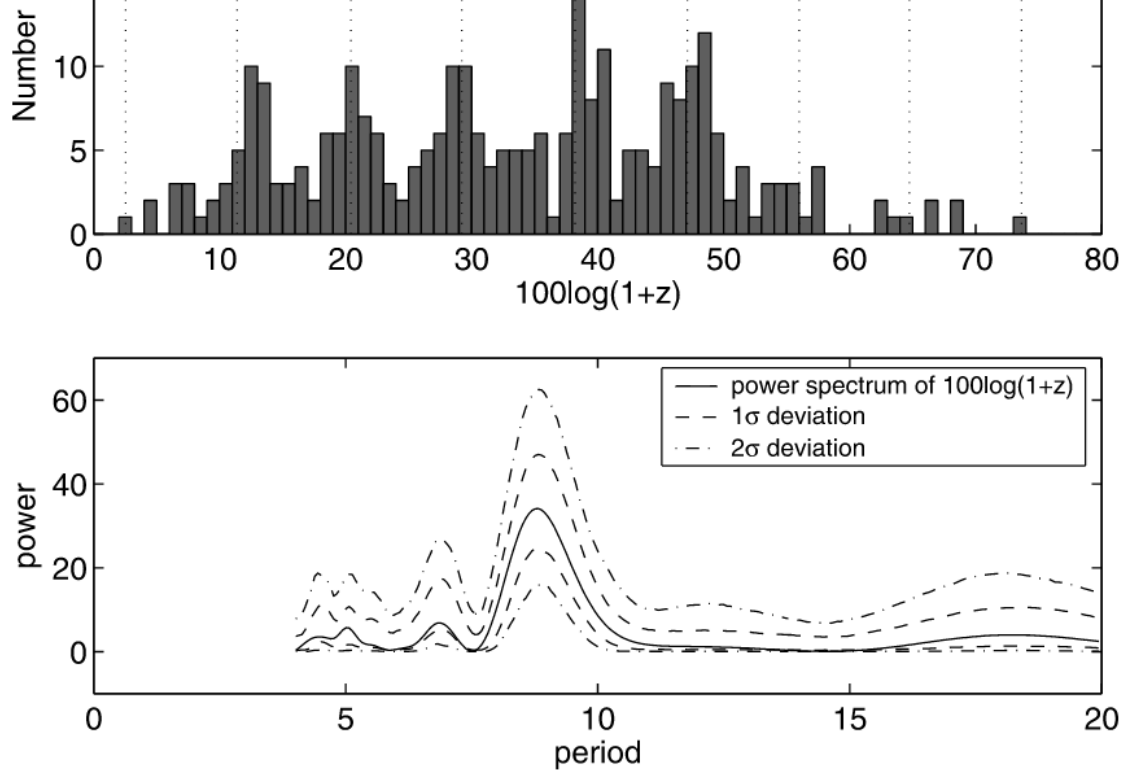
Fig. 1.—Combined QSO data set from Karlsson (1990), Burbidge & Napier (2001), and Napier & Burbidge (2003). *Top*: Histogram of redshifts of these QSOs with peaks predicted by Karlsson's formula indicated by dotted vertical lines. *Bottom*: Unwindowed power spectra of $100 \log (1 + z)$ (*solid line*) with 1 σ (*dashed lines*) and 2 σ (*dash-dotted lines*) deviations given from 1000 bootstrap simulations.

consistent with Poissonian fluctuations, i.e., there is no evidence for a periodicity at the predicted frequency in $\log (1 + z)$, or at any other frequency.

2.3. *QSO Density Contours*

After the work of Hawkins et al. (2002) on 2dF data, Arp et al. (2005) argued that the predicted periodic redshifts are apparent in the brighter 2dF quasars in the QSO density contours. We therefore use SDSS DR1 data to construct the contours defined by Arp et al. (2005), where the whole region is divided into boxes $\Delta z \times \Delta B = 0.075 \times 0.3$ in the redshift/apparent magnitude plane, and the number of quasars in each box is then counted. To show whether the predicted periodic redshifts are obscured by our coarse grid sizes, a contour with $\Delta z \times \Delta B = 0.05 \times 0.2$ is also presented for comparison. As shown in Figure 6, the peak positions are consistent in the two contour plots, and there is no evidence for redshift peaks at the predicted positions.

3. NO STRONG CONNECTION BETWEEN ACTIVE GALAXIES AND BELL'S HIGH-*z* QSOs

In Bell (2005), a high-redshift QSO sample from SDSS and a low-redshift QSO and QSO-like object sample from Hewitt & Burbidge (1993) were presented. Although the dips at redshifts of 2.7 and 3.5 have been explained as being caused by the lower efficiency of the selection algorithm at these redshifts (Richards

et al. 2002), Bell (2005) nevertheless claimed that the corresponding redshift peaks at 3.1 and 3.7 in the high-*z* SDSS QSOs come from the intrinsic redshift broadening by Doppler ejection and Hubble flow components, which favors the DIR model. Through analysis of the profiles of such peaks, Bell (2005) derived a mean cosmological components to be $z_c \sim 0.066$ for the high-*z* sample.

In the DIR model, galaxies are produced continuously through the entire age of the universe, and QSOs are assumed to be ejected from the nuclei of active galaxies and represent the first very short lived stage (10^7–10^8 yr) in the evolution of galaxies. If this is true, there must be some connection between foreground active galaxies and high-*z* QSOs beyond gravitational lensing. Here we examine the high-redshift samples taken from the SDSS data. We test the relationship between 2691 QSOs with redshifts in $\sim$2.4–4.8 and 77,426 nearby active galaxies with redshifts in $\sim$0.01–0.2 from NYU-VAGC, all of which have the highest plate quality labeled as "good" and with no redshift warning. We intercompare these two data sets to find all QSO-galaxy pairs within an angular separation corresponding to less than a given distance $D_{\mathrm{separation}}$ from several kiloparsecs to 1 Mpc at the distance of the galaxy. In some cases, there is more than one galaxy within the $D_{\mathrm{separation}}$ projected distance limit of the QSO; for these objects we take the closest galaxy in projected distance to make up the pair. Since it is suggested that all QSOs are born out of active galaxies and QSOs should be significantly fainter
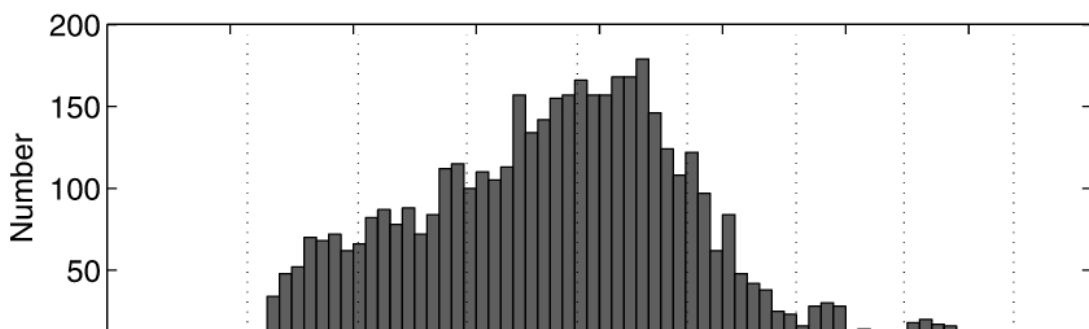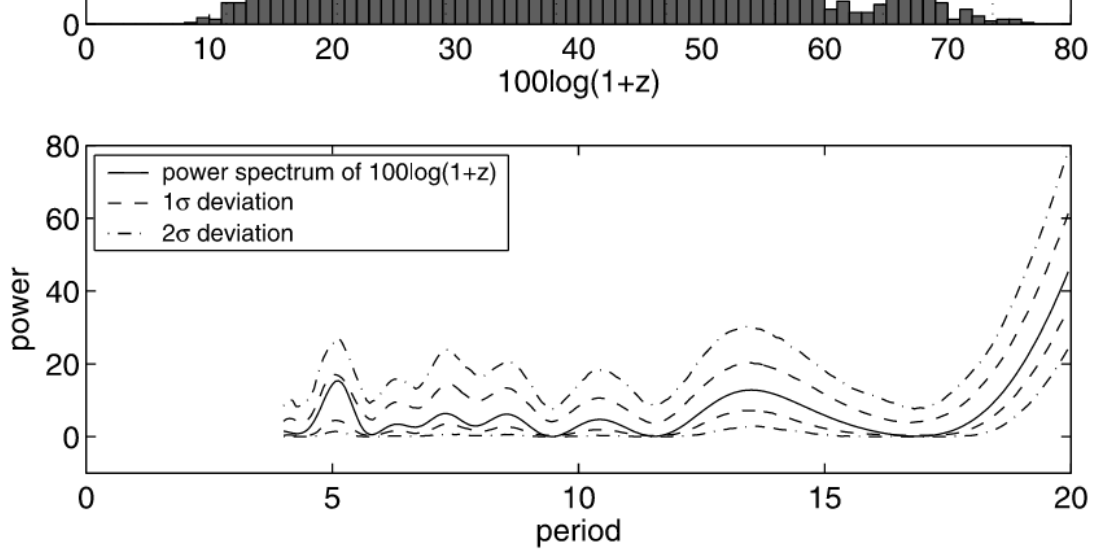
FIG. 2.—Same as Fig. 1, but for effective redshifts of 4572 QSOs paired with nearby galaxies with a projection distance less than 200 kpc.
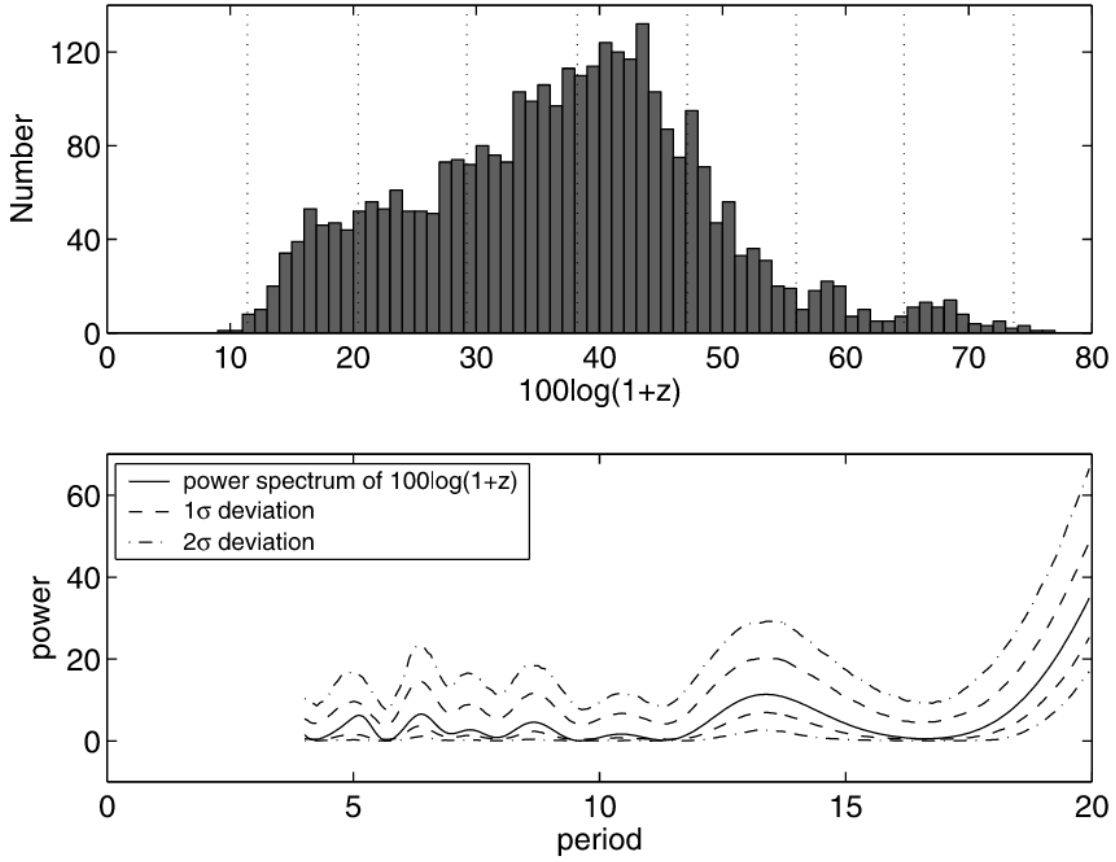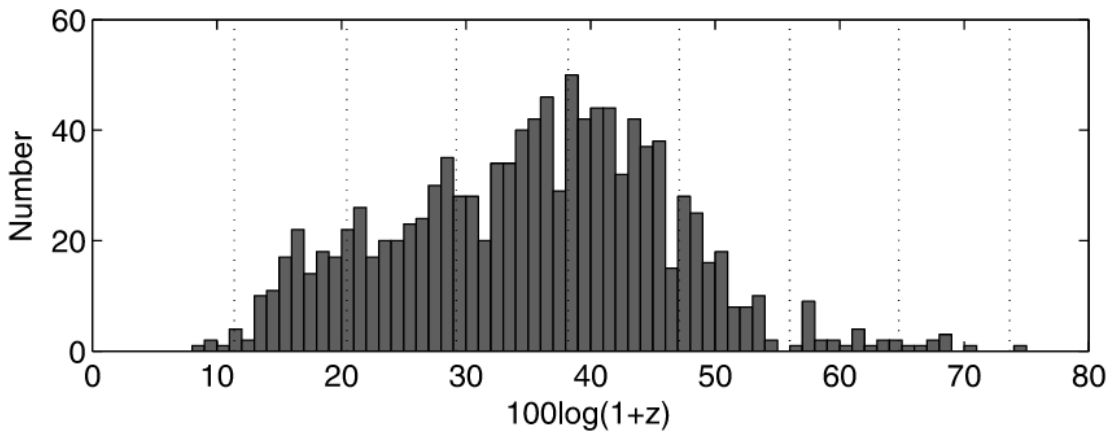

FIG. 3.—Same as Fig. 1, but for effective redshifts of 3216 QSOs paired with nearby active galaxies (star-forming or starburst galaxies) with a projection distance less than 200 kpc.
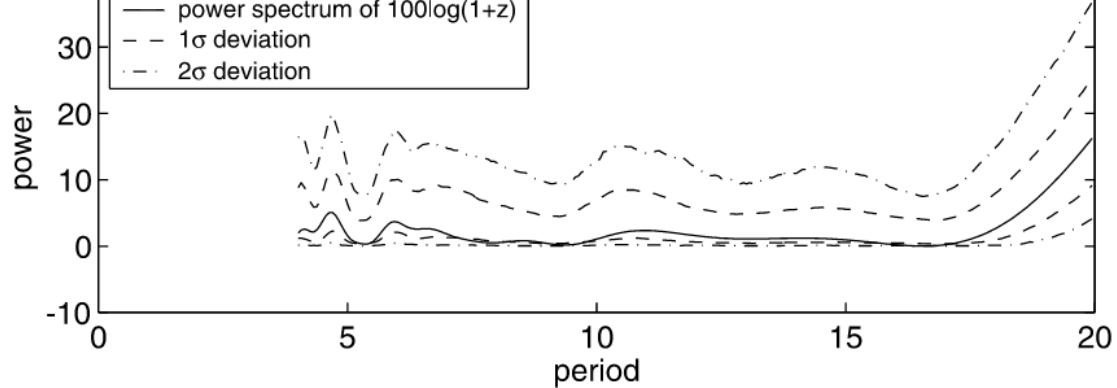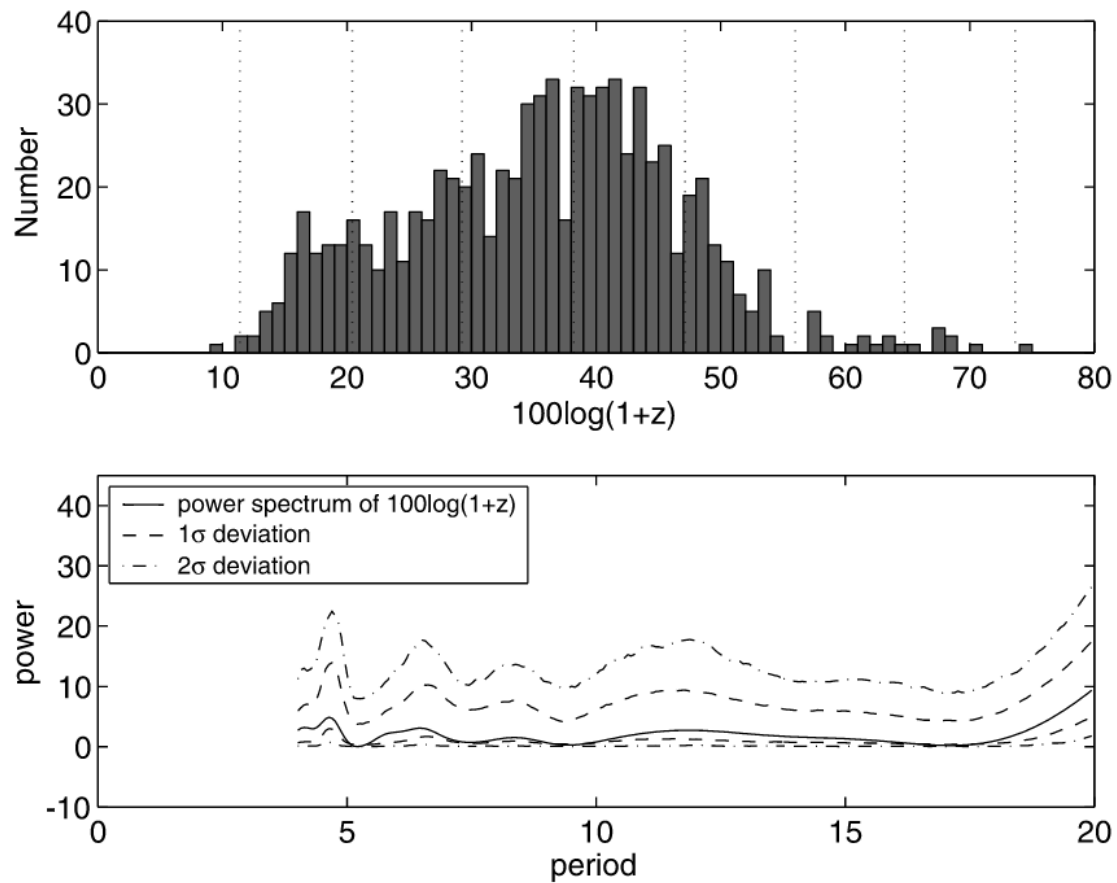
44

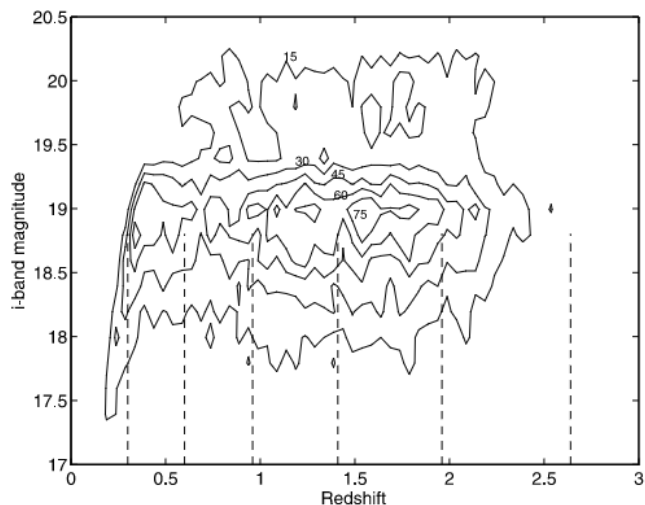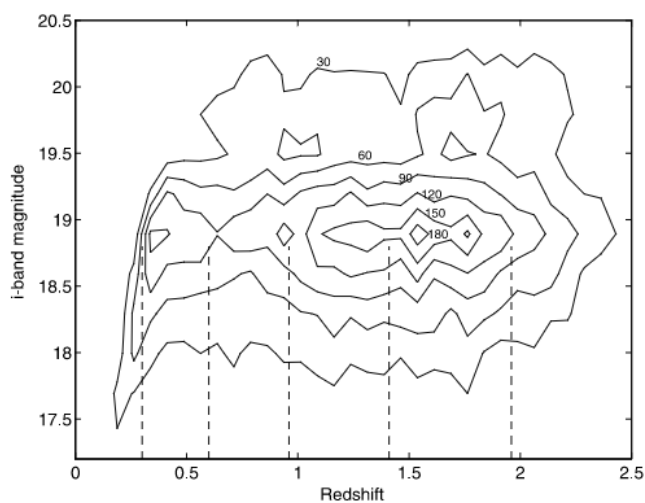Fɪɢ. 4.—Same as Fig. 1, but for effective redshifts of 958 bright QSOs ($i < 18.5$) paired with nearby galaxies with a projection distance less than 200 kpc.

Fɪɢ. 5.—Same as Fig. 1, but for effective redshifts of 671 bright QSOs ($i < 18.5$) paired with nearby active galaxies (star-forming or starburst galaxies) with a projection distance less than 200 kpc.

45

Fig. 6.—Apparent magnitude vs. measured redshift for QSOs in the SDSS DR1 catalog. In the left panel, the whole region is divided into boxes $\Delta z \times \Delta B = 0.075 \times 0.3$ in the redshift/apparent magnitude plane, while $\Delta z \times \Delta B = 0.05 \times 0.2$ in the right panel. The contours represent QSO density in steps of 180, 150, 120, 90, 60, and 30 in the left panel, while in the right panel they represent 75, 60, 45, 30, and 15, from the innermost (high density) to outermost (low density). The predicted Karlsson peaks at $z = 0.30$, 0.60, 0.96, 1.41, 1.96, and 2.64 are shown by vertical lines.
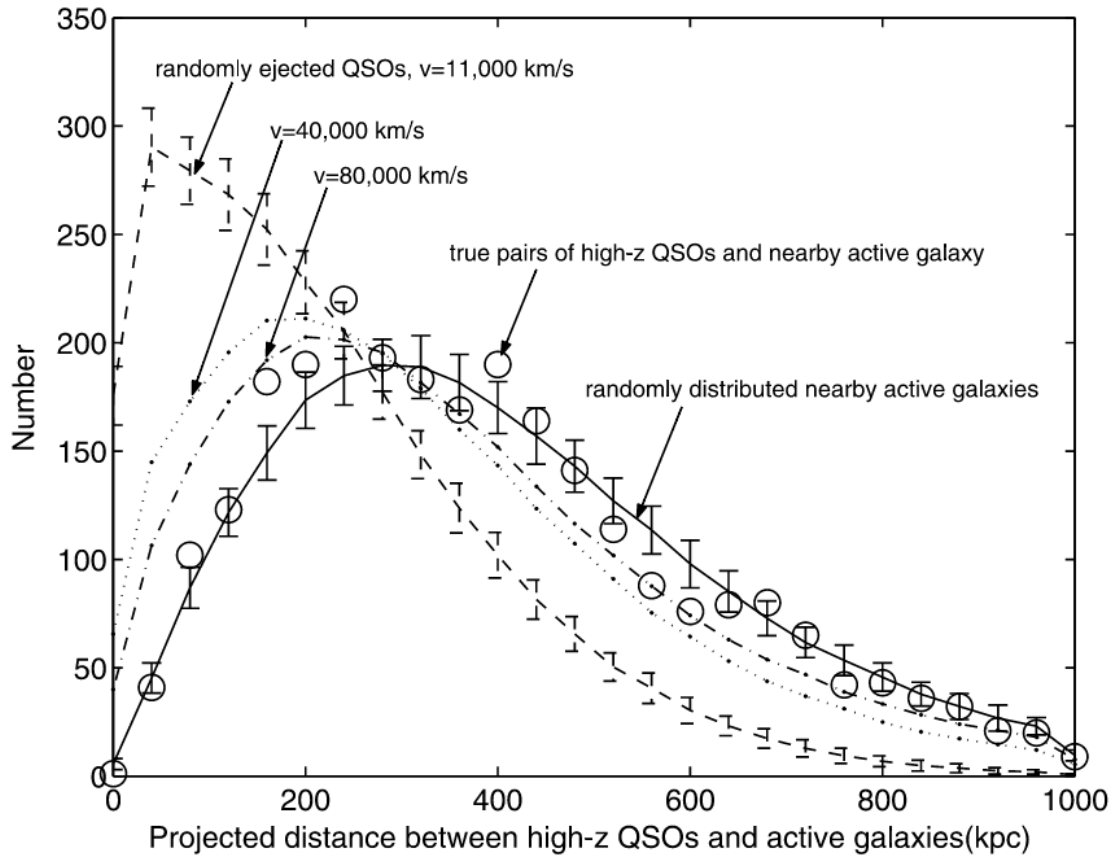
Fig. 7.—Distribution of projected distance between 2604 high-z QSOs ($2.4 < z < 4.8$) and their paired nearby active galaxies in NYU-VAGC. The circles represent "true" pairs, i.e., pairs found in the data, but not necessarily physical pairs. The solid line with error bars is the average of 200 simulations of QSOs and randomly distributed galaxies. Averages of 200 simulations of randomly ejected QSOs and active galaxies are also presented, in which QSOs are produced by ejection from randomly chosen galaxies with a uniformly distributed age in $0-10^8$ yr and three different velocities: dashed line with error bars, 11,000 km s^{-1}; dotted line with points, 40,000 km s^{-1}; and dash-dotted line with points, 80,000 km s^{-1}.
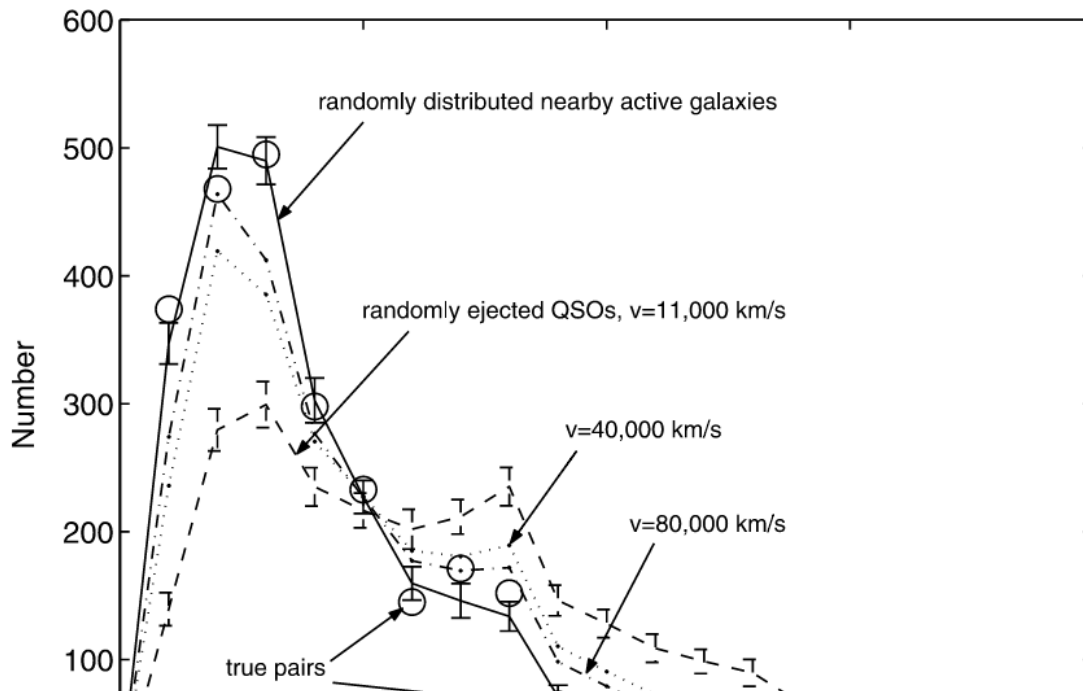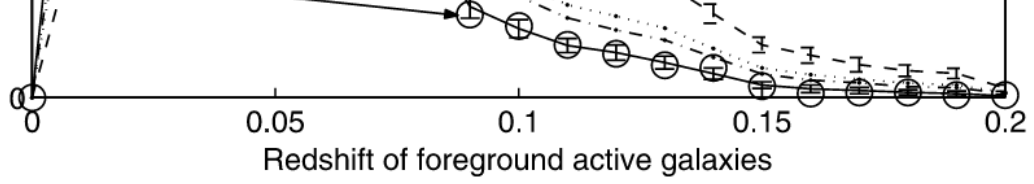
Fig. 8.—Distribution of 2604 foreground active galaxies that have at least one high-z QSO within a projected distance of 1 Mpc in NYU-VAGC. The circles represent "true" pairs. Others are as in Fig. 7.

than their parent galaxies (Bell 2005), we would not miss a considerable fraction of parent active galaxies for high-z QSOs if the DIR model is right.

The distribution of projected separation distance for all pairs is shown in Figure 7, and the redshift distribution of active galaxies in pairs with QSOs is shown in Figure 8. Both of them are consistent with random distributions, but totally different from the distribution from the ejection simulation with a ejection velocity of 11,000 km s^{-1}, which was given by Bell (2005) as a typical value, and the mean redshift of these galaxies is $z \sim 0.044$, also significantly different from Bell's result of 0.066. Here the random distributions are obtained by moving the posi-

tions of all galaxies by 1° in random directions; thus these galaxies should be completely unrelated to background QSOs. The ejection simulation is done by ejecting all QSOs from randomly selected active galaxies with three ejection velocities, 11,000, 40,000, and 80,000 km s^{-1}, and with a uniformly distributed age of $\sim 0-10^8$ yr, which is given by Bell (2005) as a typical value.

To quantitatively show the differences between simulations and "true" QSO-galaxy pairs, i.e., pairs found in the data but not necessarily physical pairs, results of χ^2 tests are given in Table 1. At the 3 σ confidence level for both distributions of projected separation distance and redshift distribution of active galaxies in pairs with QSOs, the "true" QSO-galaxy pairs are

TABLE 1

RESULTS OF χ^2 TESTS FOR THE DISTRIBUTION OF PROJECTED SEPARATION DISTANCE AND THE REDSHIFT DISTRIBUTION OF ACTIVE GALAXIES IN PAIRS WITH HIGH-z QSOs BETWEEN "TRUE" PAIRS AND SIMULATIONS

Simulations (1)	χ^{2a} (2)	χ^2/N^a (3)	p^a (4)	χ^{2b} (5)	χ^2/N^b (6)	p^b (7)
Randomly distributed galaxies	38.456	1.6720	0.023	18.818	0.9904	0.47
Ejected QSOs:						
$v = 11,000$ km s^{-1}	2560.3	111.3174	$<10^{-10}$	994.10	52.3211	$<10^{-10}$
$v = 40,000$ km s^{-1}	227.12	9.8748	$<10^{-10}$	265.31	13.9637	$<10^{-10}$
$v = 80,000$ km s^{-1}	85.496	3.7172	4.0×10^{-9}	144.37	7.5984	$<10^{-10}$

[a] Cols. (2) and (3) are for the distribution of projected separation distance. Pairs with projected separation distance less than 60 kpc (first and second points in Fig. 7) are not used in the tests to avoid the SDSS 55″ fiber constraint, and all simulations are normalized to get a minimum χ^2. The degrees of freedom are $N = 23$.

[b] Cols. (4)–(7) are for the redshift distribution of active galaxies in pairs with high-z QSOs. All of the first zero points in Fig. 8 are not used in the tests, and all simulations are normalized to get a minimum χ^2. The degrees of freedom are $N = 19$.
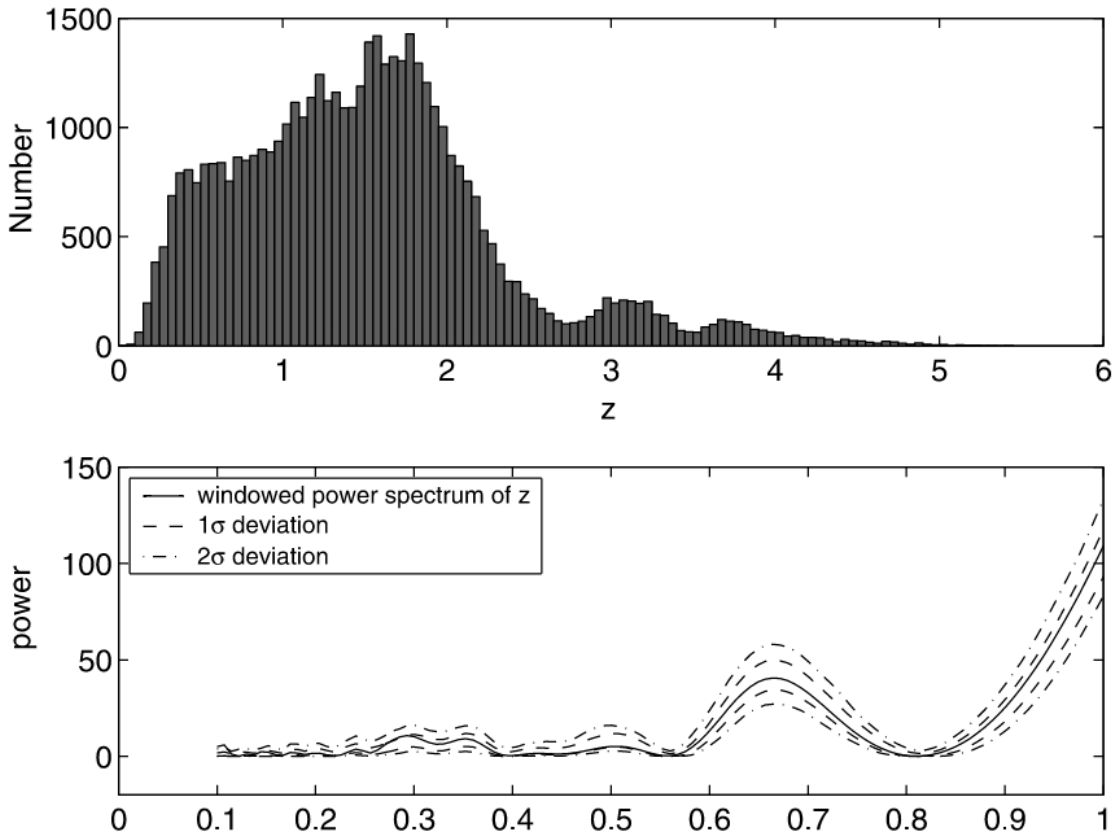
TANG & ZHANG

consistent with random distributions, but inconsistent with the ejection hypothesis with ejection velocity up to 80,000 km s^{-1}.

4. NO PERIODICITY IN z

We also analyze the periodicity in redshifts of QSOs in SDSS DR3 (Schneider et al. 2005) and 2dF (Croom et al. 2004) to investigate in a larger database of QSOs whether there is the periodicity of $\Delta z = 0.67 \pm 0.05$ predicted by the DIR model. Six data sets are used in this section: all 46,420 QSOs in SDSS DR3 (Fig. 9), 22,497 QSOs with the highest quality flag in 2dF (Fig. 10), a high-completeness (close to 100%) subsample containing 23,109 QSOs with Galactic-extinction-corrected i-band magnitude (m_i) less than 19 and redshift less than 2 in SDSS DR3 (Richards et al. 2002) (Fig. 11a), and three subsamples containing QSOs in low-completeness (less than 50%) regions in SDSS DR3: 15,696 QSOs with $m_i > 19$ and $z < 2.4$ (Fig. 11b), 19,064 QSOs with $m_i > 19$ in all redshifts (Fig. 11c), and 9763 QSOs with $z > 2$ (Fig. 11d). To reduce the edge effect produced by the truncated redshift distribution, which has a lower redshift cutoff due to the small space volume sampled and a higher redshift cutoff due to the observational flux limit (see, e.g., Hawkins et al. 2002), we follow Hawkins et al. to use the Hann function as a weighting in equation (5),

$$w_i = \frac{1}{2}\left[1 - \cos\left(\frac{2\pi x_i}{L}\right)\right], \qquad (6)$$

where L is chosen to cover the range of redshifts. Here $L = 5.4$ for the full SDSS sample, $L = 3.1$ for the 2dF sample, and

$L = 1.95$, 2.1, 5.1, and 3.4 for the four SDSS subsamples, respectively.

After smoothing off the sharp edges in the lowest and highest redshifts, a periodicity around $\Delta z = 0.67$ is detected in the full sample of SDSS QSOs, as shown in Figure 9; however, a periodicity of $\Delta z = 0.67 \pm 0.05$ or any other frequency is not found in the 2dF QSOs, as shown in Figure 10. Such a difference between these two surveys is not surprising, since the redshift-dependent spectroscopic completeness is relatively flat in 2dF (Croom et al. 2004), while in SDSS the spectroscopic completeness varies drastically at some redshifts (Richards et al. 2002). It is therefore improper to use all QSO redshifts in SDSS to probe any intrinsic periodicity without addressing selection bias. To further investigate whether such a periodicity around $\Delta z = 0.67$ in SDSS QSOs is spuriously produced by various incompleteness as function of redshift, we select a high-completeness subsample of 23,109 QSOs with $m_i < 19$ and $z < 2$ in SDSS DR3 and three subsamples containing QSOs in low-completeness regions. As shown in Figure 11, no periodicity is found in the high-completeness sample in which the power spectrum is consistent with a continuously ascending curve due to the low-frequency component of the redshift distribution, whereas in different low-completeness samples, strong periodicity always appears, but with different peak locations (0.88 in Fig. 11b, 0.67 in Fig. 11c, and 0.74 in Fig. 11d). This should be a strong indicator that the peaks in low-completeness samples are caused by different selection effects in different samples. In sum, there is no evidence for intrinsic periodicity in redshifts of QSOs.
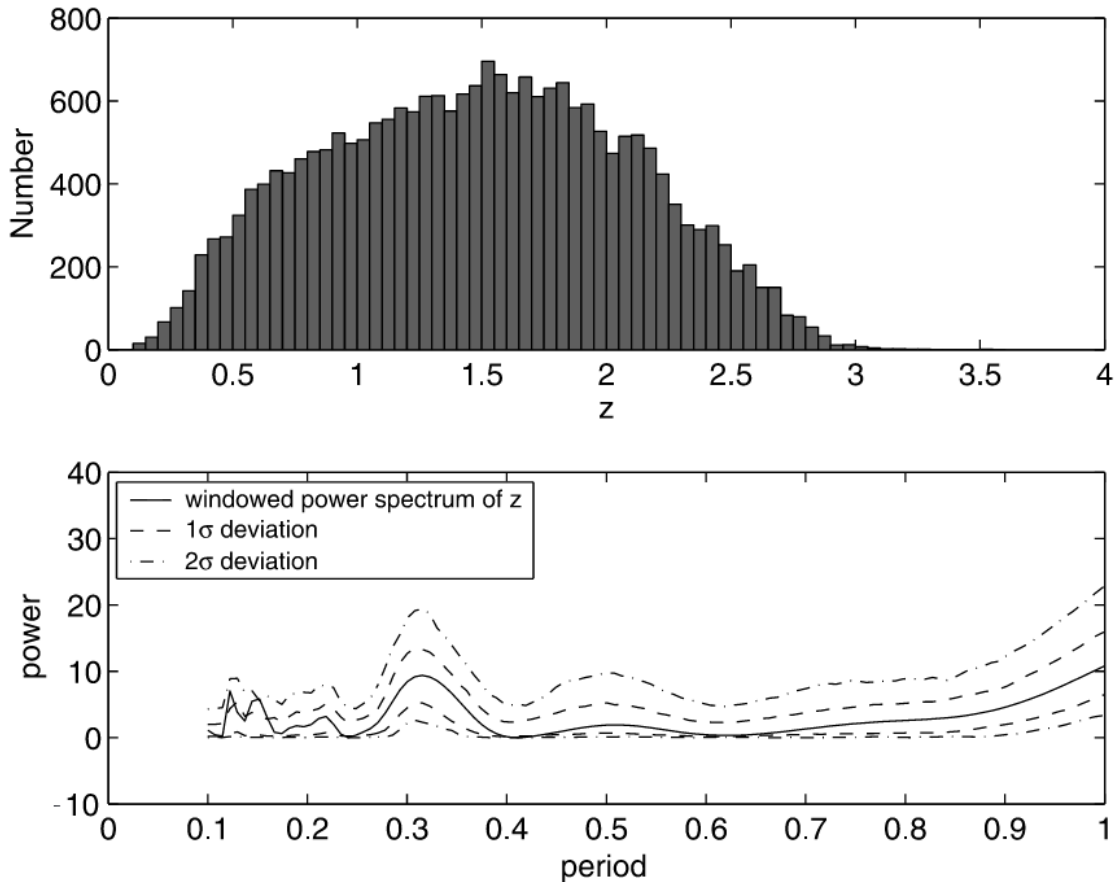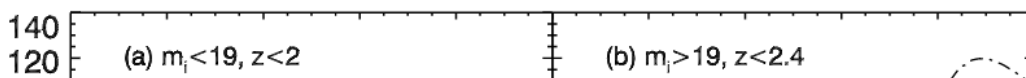

Fig. 10.—Same as Fig. 9, but for redshifts of 22,497 QSOs with the highest quality flag in 2dF.
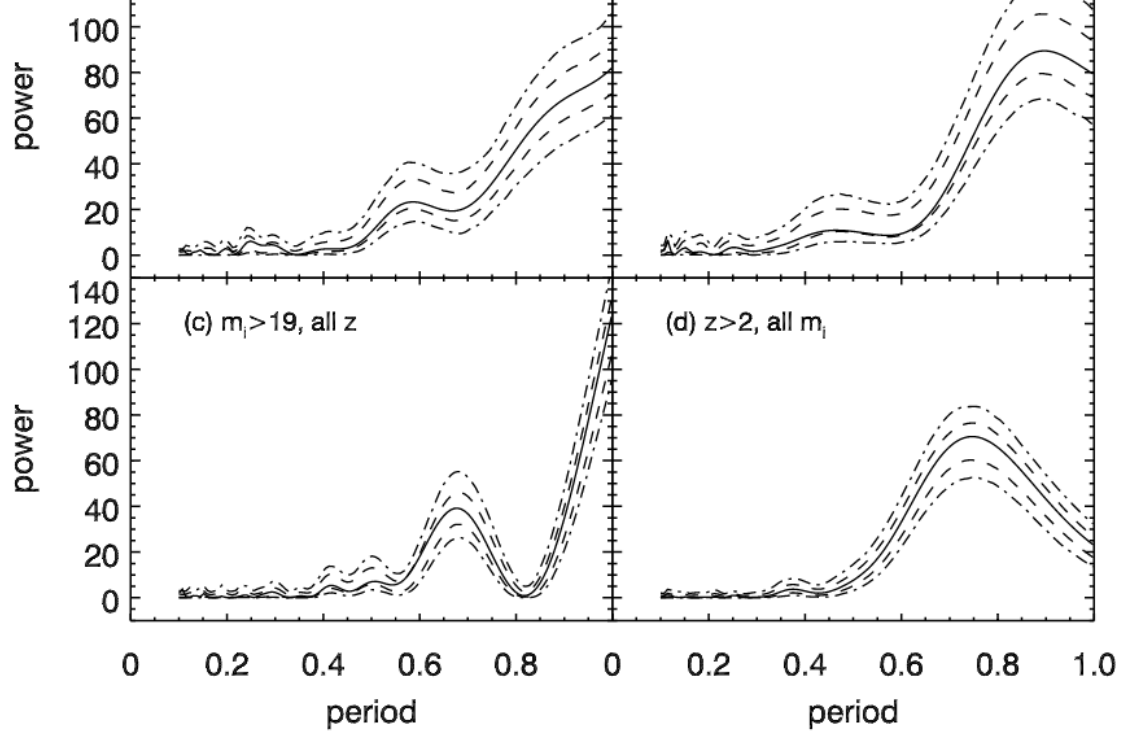
140
120 (a) $m_i < 19$, $z < 2$ (b) $m_i > 19$, $z < 2.4$

Fig. 11.—Power spectra of redshift of four subsamples from SDSS DR3. Panel (*a*) is for the high-completeness sample containing 23,109 QSOs with $m_i < 19$ and $z < 2$, and the other panels are for samples containing QSOs in low-completeness regions: (*b*) 15,696 QSOs with $m_i > 19$ and $z < 2.4$, (*c*) 19,064 QSOs with $m_i > 19$, and (*d*) 9763 QSOs with $z > 2$. The power spectra of z (*solid line*) is weighted using a Hann function with 1 σ (*dashed lines*) and 2 σ (*dash-dotted lines*) deviations given from 1000 bootstrap simulations.
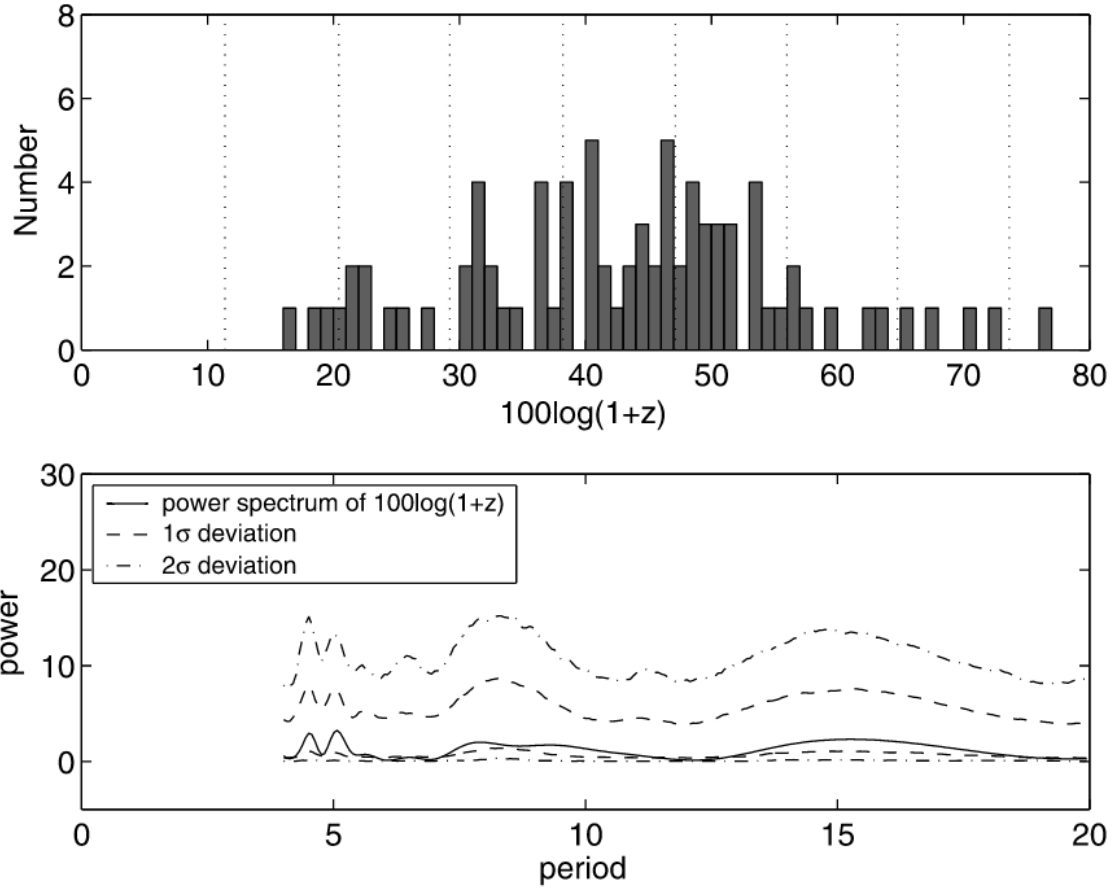
Fig. 12.—Same as Fig. 1, but for effective redshifts of 82 QSOs paired with galaxies with a projection distance less than 200 kpc, which are at least 5 mag fainter than the paired galaxies in *i* band.
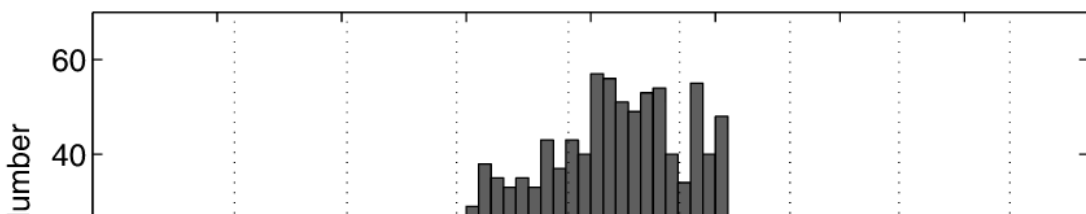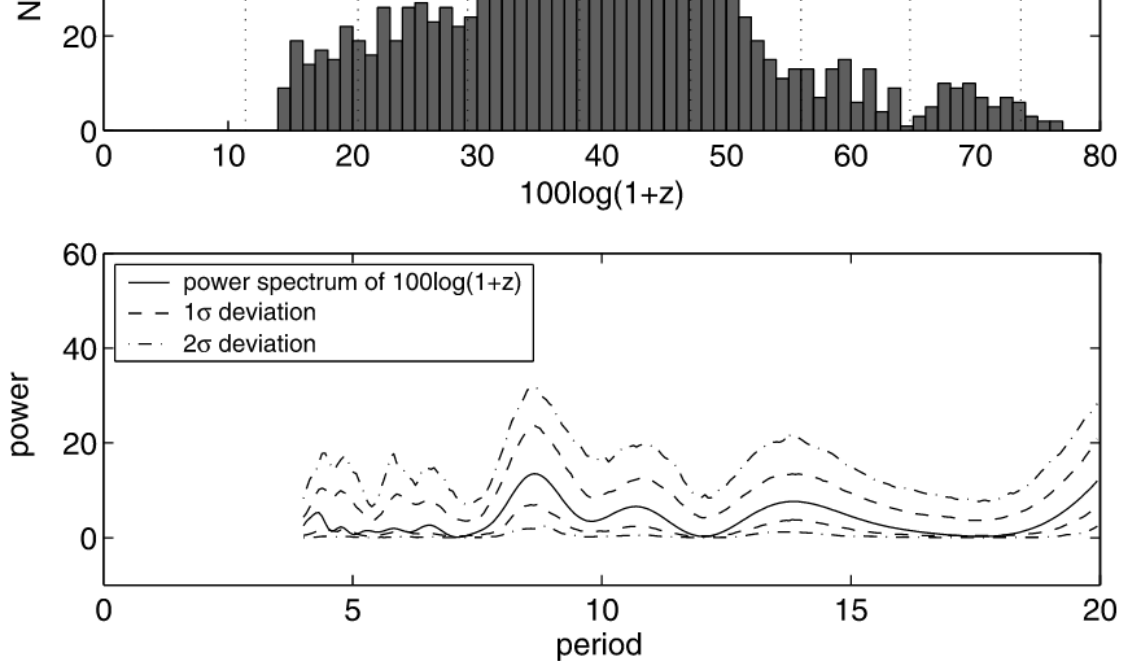
Fig. 13.—Same as Fig. 1, but for effective redshifts of 1459 QSOs paired with galaxies with a projection distance less than 200 kpc, which are at least 3 mag fainter than the paired galaxies in i band.

5. DISCUSSION AND CONCLUSION

However, one might ask whether it is because we have paired some QSOs with the wrong parent galaxies that not only do the effective redshifts of QSOs show no periodicity but also the high-z QSOs and nearby active galaxies show no strong connection. The wrong pairing indeed could happen when there is more than one galaxy within the $D_{\mathrm{separation}}$ projected distance limit of the QSO and we take the closest galaxy in projected distance to make up the pair. In the following we quantitatively examine this possibility and its effect.

For the pair-making process in § 2, the $D_{\mathrm{separation}}$ is 200 kpc, which is less than the average projection distance between QSOs and galaxies, and the percentage of cases in which there are two or more galaxies within the projected distance is 27% for QSO-nearby galaxies, 19% for QSO-active nearby galaxies, 27% for bright QSO-nearby galaxies, and 18% for bright QSO-active nearby galaxies. This means that for a majority of paired QSOs (>73%), there is only one galaxy within the given projected distance and would not be paired incorrectly; hence the claimed periodicity should have been detected in our larger samples if they did exist.

For the pair-making process in § 3, the largest $D_{\mathrm{separation}}$ is 1 Mpc, which is larger than the average projection distance between QSOs and galaxies ($\sim$400 kpc); therefore wrong-pairing may occur more frequently here. It will be even worse if the typical ejection distance is larger than the mean projection separation of QSOs and active galaxies. So would such wrong pairs result in the good agreement between ejected model and randomly generated pairs? We answer this question by making the following test. Supposing that all QSOs are ejected by randomly selected active galaxies with a given ejection velocity (11,000, 40,000, and 80,000 km s^{-1}), and with a uniformly distributed age of $\sim$0–10^8 yr, which is given by Bell (2004) as typical values, we get 200 sets of false pairs. As shown in Figures 7 and 8 and Table 1, the distribution of such simulated ejection QSO-galaxy pairs are totally different from a random distribution. We therefore conclude that the random-like distribution of QSO-active galaxy pairs could not be produced by the ejection model.

Another question is whether we miss periodicities of QSOs by setting a lower limit of $z = 0.01$ for galaxies and no constraint in the QSO-galaxy magnitude relation. Although the lower limit of $z = 0.01$, the same as in Hawkins et al. (2002), is chosen

for confidence in the derived angular distance, as well as to avoid the large projection effect of very nearby galaxies, we reanalyze SDSS DR1 QSOs and galaxies again with no redshift limits on galaxies and set the magnitude constraint that all paired QSOs should be at least 5 or 3 mag fainter than the paired galaxy. As shown in Figures 12 and 13, similar to our results in § 2.2, there is no evidence for a periodicity at the predicted frequency in $\log(1 + z)$, or at any other frequency.

In summary, using samples from SDSS and 2QZ, we demonstrate that not only is there no periodicity at the predicted frequency in $\log(1 + z)$ and z, or at any other frequency, but there is also no strong connection between foreground active galaxies and high-redshift QSOs. These results are against the hypothesis that QSOs are ejected from active galaxies or have periodic intrinsic noncosmological redshifts.

REFERENCES

Abazajian, K., et al. 2003, AJ, 126, 2081
Arp, H., Bi, H. G., Chu, Y., & Zhu, X. 1990, A&A, 239, 33
Arp, H., Roscoe, D., & Fulton, C. 2005, preprint (astro-ph/0501090)
Basu, D. 2005, ApJ, 618, L71
Bell, M. B. 2004, ApJ, 616, 738
Blanton, M. R., Lin, H., Lupton, R. H., Maley, F. M., Young, N., Zehavi, I., &
    Loveday, J. 2003, AJ, 125, 2276
———. 2005, AJ, 129, 2562
Burbidge, G. R., & Burbidge, E. M. 1967, ApJ, 148, L107
Burbidge, G. R., & Napier, W. M. 2001, AJ, 121, 21
Chu, Y., Wei, J., Hu, J., Zhu, X., & Arp, H. 1998, ApJ, 500, 596
Croom, S. M., Smith, R. J., Boyle, B. J., Shanks, T., Miller, L., Outram, P. J., &
    Loaring, N. S. 2004, MNRAS, 349, 1397
Efron, B. 1979, Ann. Stat., 7, 1
Hawkins, E., Maddox, S., & Merrifield, M. 2002, MNRAS, 336, L13
Hewitt, A., & Burbidge, G. 1993, ApJS, 87, 451
Karlsson, K. G. 1977, A&A, 58, 237
———. 1990, A&A, 239, 50
Napier, W. M., & Burbidge, G. 2003, MNRAS, 342, 601
Richards, G. T., et al. 2002, AJ, 123, 2945
Schneider, D. P., et al. 2003, AJ, 126, 2579
———. 2005, AJ, 130, 367
Strauss, M. A., et al. 2002, AJ, 124, 1810